DMD Fast Forward. Published on November 5, 2012 as DOI: 10.1124/dmd.112.049114
DMD Fast Forward. Published on November 5, 2012 as doi: 10.1124/dmd.112.049114
This article has not been copyedited and formatted. The final version may differ from this version.

DMD #049114

TITLE: Prediction of Crizotinib-Midazolam Interaction using the Simcyp Population-based Simulator: Comparison of CYP3A Time-Dependent Inhibition between Human Liver Microsomes versus Hepatocytes

AUTHORS: Jialin Mao, Theodore R. Johnson, Zhongzhou Shen and Shinji Yamazaki

ADDRESS: Pharmacokinetics, Dynamics and Metabolism (J.M., T.R.J., Z.S., S.Y.), Pfizer Worldwide Research & Development, San Diego, California

Downloaded from dmd.aspetjournals.org at ASPET Journals on February 7, 2023

Copyright 2012 by the American Society for Pharmacology and Experimental Therapeutics.

DMD Fast Forward. Published on November 5, 2012 as DOI: 10.1124/dmd.112.049114
This article has not been copyedited and formatted. The final version may differ from this version.

RUNNING TITLE: Prediction of Crizotinib-Midazolam Interaction

CORRESPONDING AUTHOR:

Shinji Yamazaki, Ph.D.

Pharmacokinetics, Dynamics and Metabolism, La Jolla Laboratories

Pfizer Worldwide Research and Development

10777 Science Center Drive, San Diego, CA 92121, USA

Tel: 858-622-8050 Fax: 858-622-8252

E-mail: shinji.yamazaki@pfizer.com

Number of Text Pages:	43
Number of Tables:	4
Number of Figures:	7
Number of References:	37
Number of Words in the Abstract:	250
Number of Words in the Introduction:	750
Number of Words in the Discussion:	1492

Downloaded from dmd.aspetjournals.org at ASPET Journals on February 7, 2023

DMD Fast Forward. Published on November 5, 2012 as DOI: 10.1124/dmd.112.049114
This article has not been copyedited and formatted. The final version may differ from this version.

ABBREVIATIONS:

AUC, area under the plasma concentration-time curve; $C_{inlet,u}$, unbound hepatic inlet concentration; C_{max}, maximum plasma concentration; $C_{sys,u}$, unbound systemic concentration; CL_{int}, hepatic intrinsic clearance; DDI, drug-drug interactions; EI, enzyme induction; f_m, fraction metabolized by an enzyme; K_i, inhibition constant; K_I, inactivation constant; k_{inact}, maximum inactivation rate constant; $K_{I,app}$, apparent inactivation constant; k_{deg}, degradation rate constant; k_{obs}, apparent inactivation rate constant; k_p, tissue to plasma partition coefficient; f_u, unbound fraction; HEP, human hepatocytes; HLM, human liver microsomes; HSP, human hepatocytes suspended in human plasma; PBPK, physiologically-based pharmacokinetics; $P_{eff,man}$, projected human jejunum permeability; R_{bp}, blood-to-plasma ratio; RI, reversible inhibition; TDI, time dependent inhibition; t_{max}, time to reach maximum plasma concentration; V_{ss}, volume of distribution at steady-state

Downloaded from dmd.aspetjournals.org at ASPET Journals on February 7, 2023

DMD Fast Forward. Published on November 5, 2012 as DOI: 10.1124/dmd.112.049114
This article has not been copyedited and formatted. The final version may differ from this version.

ABSTRACT

Crizotinib (Xalkori®) is an orally available potent inhibitor of multiple tyrosine kinases including anaplastic lymphoma kinase and mesenchymal-epithelial transition factor. Objectives of the present study were to: 1) characterize crizotinib time-dependent inhibition (TDI) potency for CYP3A in human liver microsomes (HLM) and cryopreserved human hepatocytes suspended in plasma (HSP), 2) characterize crizotinib enzyme induction potency on CYP3A4 in cryopreserved human hepatocytes (HEP), 3) predict crizotinib steady-state plasma concentrations in patients (e.g., autoinhibition and autoinduction) using the mechanistic dynamic model, Simcyp population-based simulator, and 4) predict a clinical crizotinib-midazolam interaction using the dynamic model as well as the static mathematical model. Crizotinib inactivation constant (K_I) and maximum inactivation rate constant (k_{inact}) for TDI were estimated as, respectively, 0.37 μM and 6.9 h^{-1} in HLM and 0.89 μM and 0.78 h^{-1} in HSP. Thus, crizotinib inactivation efficiency (k_{inact} / K_I) was approximately 20-fold lower in HSP relative to HLM. Crizotinib E_{max} and EC_{50} for CYP3A4 induction (measured as mRNA expression) were estimated as 6.4- to 29-fold and 0.47 to 3.1 μM, respectively. Based on these in vitro parameters, the predicted crizotinib steady-state area under plasma concentration-time curve (AUC) with HLM-TDI was 2.1-fold higher than the observed AUC whereas that with HSP-TDI was consistent with the observed result (≤1.1-fold). The increase in midazolam AUC with co-administration of crizotinib (21-fold) was significantly over-predicted using HLM-TDI whereas the prediction using HSP-TDI (3.6-fold) was consistent with the observed result (3.7-fold). Collectively, the present study demonstrated the value of HSP to predict in vivo CYP3A-mediated drug-drug interaction.

Downloaded from dmd.aspetjournals.org at ASPET Journals on February 7, 2023

DMD Fast Forward. Published on November 5, 2012 as DOI: 10.1124/dmd.112.049114
This article has not been copyedited and formatted. The final version may differ from this version.

INTRODUCTION

A clinically relevant drug-drug interaction (DDI) is generally considered a modification of pharmacological and/or toxicological effects of one drug (object) by another drug (precipitant). In many cases, DDI can be attributed to modulation of drug metabolizing enzymes, particularly CYP3A, as these are the most abundantly expressed in the liver and intestines (Shimada et al., 1994; Slaughter and Edwards, 1995). The enzyme inhibition mechanism can be categorized as reversible (competitive, uncompetitive or noncompetitive) inhibition (RI) or time-dependent (mechanism-based or metabolism-based) inhibition (TDI). For in vitro TDI evaluation, an inactivation constant (K_I) and a maximum inactivation rate constant (k_{inact}) are typically determined in human liver microsomes (HLM) (Grimm et al., 2009; Zimmerlin et al., 2011), and these kinetic parameters are used to predict potential in vivo DDI (Kanamitsu et al., 2000; Mayhew et al., 2000; Obach et al., 2007). In addition to HLM, TDI evaluation in human hepatocytes (HEP) has recently been reported for the known CYP3A time-dependent inhibitors such as diltiazem, erythromycin and ritonavir (Zhao et al., 2005; Xu et al., 2009; Chen et al., 2011; Kirby et al., 2011). HEP are also extensively used for the evaluation of enzyme induction (EI) for CYPs (Chu et al., 2009). Compared to HLM, HEP are intact cellular systems containing a full complement of phase I/II metabolizing enzymes and transporter proteins (Di et al., 2012). The presence of cell membranes in HEP is important in maintaining the effects of active uptake/efflux transporters and passive diffusion on intracellular drug concentration; therefore, these factors may substantially affect the determination of enzyme kinetic parameters such as K_I and k_{inact}. Generally, the known CYP3A inhibitors showed a less potent TDI in HEP relative to

Downloaded from dmd.aspetjournals.org at ASPET Journals on February 7, 2023

DMD Fast Forward. Published on November 5, 2012 as DOI: 10.1124/dmd.112.049114
This article has not been copyedited and formatted. The final version may differ from this version.

HLM, which have yielded an impact on the in vivo DDI prediction (Xu et al., 2009; Chen et al., 2011; Kirby et al., 2011). Furthermore, it has been reported that cryopreserved human hepatocytes suspended in plasma (HSP), compared to those in protein-free media, showed better DDI predictions for some of CYP inhibitors (Mao et al., 2011; Mao et al., 2012).

Recently, there has been a growing interest in physiologically-based pharmacokinetic (PBPK) models, where each physiological compartment (i.e., organ or tissue defined by a tissue volume) is connected with blood flow. The PBPK model provides disposition profiles to be predicted from physico- and bio-chemical properties of compounds (Jones et al., 2006; Lave et al., 2007; Nestorov, 2007). This dynamic approach is increasingly being employed in drug discovery and development setting to predict PK and DDI potential in the clinic. Traditionally, DDI predictions have been performed with static mathematical models using various inhibitor concentrations such as hepatic inlet or outlet concentrations in total (protein bound plus unbound) or unbound form (Mayhew et al., 2000; Obach et al., 2007; Fahmi et al., 2009; Boulenc and Barberan, 2011; Mao et al., 2012). In these reports, hepatic DDI magnitudes for RI were reasonably predicted using the projected unbound portal vein (or hepatic inlet) concentration ($C_{inlet,u}$) whereas the use of unbound systemic (or hepatic outlet) concentration ($C_{sys,u}$) yielded better prediction for TDI and EI compared to $C_{inlet,u}$. Based on advancements in the field, the Food and Drug Administration (FDA) has recently issued a revised draft DDI guidance for industry (FDA, 2012), which emphasizes the use of an integrated approach such as static mathematical model or mechanistic dynamic PBPK models to simultaneously utilize these DDI mechanisms (e.g., TDI, EI and RI) to

Downloaded from dmd.aspetjournals.org at ASPET Journals on February 7, 2023

DMD Fast Forward. Published on November 5, 2012 as DOI: 10.1124/dmd.112.049114
This article has not been copyedited and formatted. The final version may differ from this version.

predict potential clinical DDI of new chemical entities. In many cases, an inhibitor concentration used for DDI prediction with general PBPK models is considered to be comparable to $C_{sys,u}$ at equilibrium since the tissue compartments are assumed to be perfusion-limited without any diffusion barrier.

Crizotinib (Xalkori®; PF02341066) was identified as an orally available potent inhibitor of multiple tyrosine kinases including anaplastic lymphoma kinase and mesenchymal-epithelial transition factor (Fig. 1). Crizotinib was recently approved by FDA for the treatment of patients with locally advanced or metastatic non-small cell lung cancer that is anaplastic lymphoma kinase-positive as detected by an FDA-approved test. It has been reported that crizotinib is a substrate of CYP3A (Johnson et al., 2011a). Objectives of the present study were to: 1) characterize crizotinib TDI potency on CYP3A in HLM and HSP, 2) characterize crizotinib EI potency in cryopreserved HEP, 3) predict crizotinib steady-state plasma concentrations in patients using the mechanistic dynamic model, and 4) predict a clinical crizotinib-midazolam interaction, utilizing the mechanistic dynamic model as well as the static mathematical model. The dynamic model used was a commercially available Simcyp population-based dynamic simulator (Jamei et al., 2009).

Downloaded from dmd.aspetjournals.org at ASPET Journals on February 7, 2023

DMD Fast Forward. Published on November 5, 2012 as DOI: 10.1124/dmd.112.049114
This article has not been copyedited and formatted. The final version may differ from this version.

Materials and Methods

Materials

Crizotinib ((R)-3-[1-(2,6-dichloro-3-fluoro-phenyl)-ethoxy]-5-(1-piperidin-4-yl-1H-pyrazol-4-yl)-pyridin-2-ylamine), chemical purity >99%) was synthesized by Pfizer Worldwide Research and Development (San Diego, CA) (Cui et al., 2011). Pooled HLM from 50 individual donors (30 males and 20 females) were prepared and characterized at XenoTech LLC (Lenexa, KS, USA). Cryopreserved HEP suspension (3 males and 2 females) and InVitro GRO^{TM} HT Medium were obtained from Celsis In Vitro Technologies, Inc. (Baltimore, MD). Human plasma (heparin as anti-coagulant) was obtained from Lampire Biological Laboratories, Inc. (Pipersville, PA). HEP maintenance medium was obtained from Lonza, Inc. (Walkersville, MD). Midazolam, 1'-hydroxymidazolam (1'-OH midazolam) and [$^{13}C_3$]-1'-hydroxymidazolam (internal standard) were obtained from BD Gentest (Woburn, MA). Glucose-6-phosphate and glucose-6-phosphate dehydrogenase were from Sigma-Aldrich. All other commercially available reagents and solvents were of either analytical or high performance liquid chromatography (HPLC) grade.

Crizotinib TDI Assay in HLM

A two-step incubation scheme was used to analyze the inhibition of midazolam hydroxylation by crizotinib in HLM. Crizotinib at final concentrations of 0.3 to 10 μM (0.1% of final DMSO concentration) was preincubated with HLM (0.5 mg/mL) and NADPH (1 mM) at 37°C for 0, 5, 10 and 20 minutes. The incubation mixture was diluted (1:10) with buffer containing NADPH (1 mM), and midazolam (10 μM) was added for an additional 3 minute incubation period to quantify 1'-hydroxymidazolam as the remaining

Downloaded from dmd.aspetjournals.org at ASPET Journals on February 7, 2023

DMD Fast Forward. Published on November 5, 2012 as DOI: 10.1124/dmd.112.049114
This article has not been copyedited and formatted. The final version may differ from this version.

CYP3A activity. The incubation was then terminated by the addition of 100 µL of acetonitrile/methanol (3:1 v/v) containing 3% formic acid and the internal standard (0.1 µM). The incubations were performed in duplicate. Samples were centrifuged at 2000*g* for 20 minutes and an aliquot of the supernatant was analyzed by liquid-chromatography tandem mass spectrometry (LC-MS/MS).

Crizotinib TDI Assay in HSP

Crizotinib TDI potency was evaluated in HSP following a similar study design as reported previously (Mao et al., 2011). Briefly, the final crizotinib concentrations used in the incubation mixture were 0.13 to 100 µM (0.5% of final methanol concentration). Incubations were performed in duplicate. A total of 25 µl of stock cryopreserved HEP (prepared in human plasma as 2×10^6 cells/ml) were added to 50 µl of human plasma containing crizotinib and incubated for 0, 10 and 20 min (37°C, 5% CO_2) before the addition of midazolam. Midazolam in human plasma (25 µl) at final concentration of 30 µM was added to the incubation mixture followed by a 35-min incubation to quantify 1'-hydroxymidazolam as the remaining CYP3A activity. The final concentration of HEP was 0.5×10^6 cells/mL. Reactions were terminated by adding 200 µL of acetonitrile/methanol (3:1 v/v) containing the internal standard (0.15 µM). Samples were centrifuged at 2000*g* for 20 minutes and an aliquot of the supernatant was analyzed by LC-MS/MS.

Crizotinib EI Assay in Cryopreserved HEP

Crizotinib CYP3A4 EI potency was evaluated in cryopreserved HEP from three donors (lot Hu4026, Hu8020 and HIE) using a procedure described previously (Fahmi et al., 2008). Briefly, cryopreserved HEP (3.5×10^5 viable cells per 0.5 mL of plating

Downloaded from dmd.aspetjournals.org at ASPET Journals on February 7, 2023

DMD Fast Forward. Published on November 5, 2012 as DOI: 10.1124/dmd.112.049114
This article has not been copyedited and formatted. The final version may differ from this version.

medium in each well of collagen I-precoated 24-well plates) were incubated for 24 hours (37°C, 95% relative humidity, 5% CO_2) before the addition of crizotinib (0.1% of final DMSO concentration). The cells were treated with crizotinib at final concentrations of 0.25 to 7 μM daily for three consecutive days. Quantification of CYP3A4 mRNA was performed using the TaqMan two-step RT-PCR method, and the relative quantity of the target CYP3A4 gene compared with the endogenous control was determined by the ΔΔCT method. An effect of crizotinib on cell viability was assessed using the WST-1 Cell Proliferation reagent.

LC-MS/MS Analysis for Midazolam Metabolite

Concentrations of the CYP3A-mediated metabolite of midazolam, 1'-hydroxymidazolam, in the in vitro TDI assays were determined by an LC-MS/MS method after the protein precipitation. The LC-MS/MS system consisted of Shimadzu LC-10ADvp pumps (Shimadzu, Columbia, MD), a CTC PAL autosampler (Leap Technologies, Carrboro, NC), and a Sciex API 4000 mass spectrometer (Sciex, Foster City, CA) equipped with a turbo ion spray source. Chromatographic separation was achieved by a reverse-phase column (Agilent Zorbax SB-Phenyl, 5 μm, 50 × 2.1 mm column, Agilent, Santa Clara, CA) with a mobile phase consisting of water with 0.1% formic acid (mobile phase A) and acetonitrile with 0.1% formic acid (mobile phase B) at a flow rate of 0.8 mL/min. The injection volume was 5 μL. Analytes were eluted using a step gradient from 1 to 40% mobile phase B over 3 minutes, and then increased to 90% in the next 0.01 minutes. Mobile phase B was held at 90% from 3.01 to 3.50 minutes, and the column was re-equilibrated to 1% over another 0.5 minutes. The MS was operated in the positive ionization mode using multiple reaction monitoring at specific parent ion →

Downloaded from dmd.aspetjournals.org at ASPET Journals on February 7, 2023

DMD Fast Forward. Published on November 5, 2012 as DOI: 10.1124/dmd.112.049114
This article has not been copyedited and formatted. The final version may differ from this version.

product ion transitions of *m/z* 342→203 for 1'-hydroxymidazolam and 345 →171 for [$^{13}C_3$]-1'-hydroxymidazolam (IS). The dynamic range of the assay ranged from 7.5 to 2540 nM. The back calculated calibration standard concentrations were within ±15% of their nominal concentrations with coefficients of variation of less than 15%. No significant carryover and matrix effects were observed in the study.

Estimation of Crizotinib TDI Kinetic Parameters

To determine TDI kinetic parameters (i.e., K_I and k_{inact}) in the HLM assay, the apparent inactivation rate constant (k_{obs}) for each crizotinib concentration ([*I*]) was first estimated from the slope of initial linear decline of CYP3A remaining activity on a natural logarithmic scale over the preincubation time. Apparent K_I ($K_{I,app}$) and k_{inact} values were then determined by solving the following nonlinear equation (Mayhew et al., 2000):

$$k_{obs} = k_{inact} \cdot [I]/(K_{I,app} + [I]) \quad (1)$$

Subsequently, for prediction purpose, an estimate for K_I was calculated from $K_{I,app}$ following the correction for in vitro non-specific binding in microsomes ($f_{u,mic}$), which was measured by the equilibrium dialysis method (Yamazaki et al., 2011).

In the HSP assay, the previously reported mathematical equations incorporating reversible (eq. 2), irreversible (eq. 3), or both reversible and irreversible inhibitions (eq. 4) were employed to estimate the apparent reversible inhibition constant ($K_{i,app}$) and/or TDI parameters ($K_{I,app}$ and k_{inact}) by simultaneously fitting three IC_{50} curves obtained from different incubation times using a weighted nonlinear regression analysis (Mao et al., 2011):

Downloaded from dmd.aspetjournals.org at ASPET Journals on February 7, 2023

DMD Fast Forward. Published on November 5, 2012 as DOI: 10.1124/dmd.112.049114
This article has not been copyedited and formatted. The final version may differ from this version.

$$\frac{Vi_t}{Vc_t} = \frac{[S] \cdot V_{max,t}}{(K_{m,MDZ} \cdot (1 + [I]/K_{i,app}) + [S]) \cdot Vc_t} \quad (2)$$

$$\frac{Vi_t}{Vc_t} = \frac{[S] \cdot V_{max,t} \cdot e^{-k_{inact} \cdot [I] \cdot t/(K_{I,app} + [I])}}{(K_{m,MDZ} + [S]) \cdot Vc_t} \quad (3)$$

$$\frac{Vi_t}{Vc_t} = \frac{[S] \cdot V_{max,t} \cdot e^{-k_{inact} \cdot [I] \cdot t/(K_{I,app} + [I])}}{(K_{m,MDZ} \cdot (1 + [I]/K_{i,app}) + [S]) \cdot Vc_t} \quad (4)$$

where, t is a total incubation time of a preincubation (0, 10 or 20 minutes) with an inhibitor followed by a 35-min incubation with midazolam, Vi_t represents the 1'-OH midazolam formation rate at a given inhibitor concentration during total incubation time, Vc_t represents the 1'-OH midazolam formation rate of vehicle control (no inhibitor) during total incubation time, $K_{m,MDZ}$ is the Michaelis-Menten constant for 1'-OH midazolam formation in HSP (55 μM total corresponding to 2 μM free), $V_{max,t}$ represents maximum 1'-OH midazolam formation rate, [I] is the nominal inhibitor concentration, and [S] is the final incubation concentration of midazolam (30 μM).

The ratio of Vi_t and Vc_t normalized the baseline for the enzyme activity at the designated incubation time. Model selection was based on a number of criteria such as Akaike information criterion, estimates for each parameters and standard errors. Finally, an estimate for $K_{I,app}$ was converted to K_I (as the input for Simcyp) following the correction for the unbound fraction in plasma ($f_{u,plasma}$),which was measured by the equilibrium dialysis method (Yamazaki et al., 2011).

Prediction of Crizotinib and Midazolam Pharmacokinetics with Simcyp

Physicochemical and in vitro pharmacokinetic parameters of crizotinib used for DDI prediction are summarized in Table 1. Based on these parameters, two compound files of crizotinib were created in Simcyp (version 11.1): one with the TDI parameters

Downloaded from dmd.aspetjournals.org at ASPET Journals on February 7, 2023

DMD Fast Forward. Published on November 5, 2012 as DOI: 10.1124/dmd.112.049114
This article has not been copyedited and formatted. The final version may differ from this version.

from HLM (henceforth referred to as CRZ-HLM) and the other with the TDI parameters from HSP (henceforth referred to as CRZ-HSP). The only difference in these two crizotinib Simcyp files was the TDI kinetic parameter value (K_I and k_{inact}). Crizotinib in vitro inhibitory effect on CYP3A (i.e., RI) using midazolam as a probe substrate was negligible with IC_{50} value of >30 μM (FDA, 2011). Crizotinib EI parameters (E_{max} and EC_{50}) estimated from three individual cryopreserved HEP were normalized to 2.4-fold and 0.84 μM, respectively, with the rifampin data (mean E_{max} of 90-fold and EC_{50} of 0.57 μM) by the induction calibrator of prediction tool box implemented in Simcyp. These EI parameters were also incorporated into both CRZ-HLM and CRZ-HSP files.

Simcyp simulations of crizotinib plasma concentration-time profiles were performed by a full-PBPK model with a first-order absorption rate constant (k_a) based upon the clinically observed plasma concentrations in healthy volunteers (n = 14) after a single 50-mg intravenous 2-hour infusion or a single 250-mg oral administration. These single-dose clinical studies of crizotinib were conducted in a crossover design with a washout period of at least 14 days (FDA, 2011). In the Simcyp absorption model, k_a values were set to predict clinically observed time to reach maximum plasma concentration (t_{max}), and an unbound fraction in the gut ($f_{u,gut}$) was assumed to be equal to an unbound fraction in blood ($f_{u,blood}$) calculated from $f_{u,plasma}$ and blood-to-plasma ratio (R_{bp}). The blood flow term (Q_{gut}) of crizotinib in the "Q_{gut}" model was estimated to be 4.0 L/h from crizotinib physicochemical properties. Using a retrograde model implemented in Simcyp, hepatic intrinsic clearance (CL_{int}) was back-calculated from the in vivo intravenous plasma clearance (47 L/h) determined in the single intravenous infusion study as mentioned above (FDA, 2011). Crizotinib renal clearance was

Downloaded from dmd.aspetjournals.org at ASPET Journals on February 7, 2023

DMD Fast Forward. Published on November 5, 2012 as DOI: 10.1124/dmd.112.049114
This article has not been copyedited and formatted. The final version may differ from this version.

negligible in humans and the fraction metabolized by CYP3A4 ($f_{m,CYP3A4}$) was suggested to be 0.8 based on the in vitro CYP phenotyping and the human mass-balance study with [^{14}C]crizotinib (Johnson et al., 2011a; Johnson et al., 2011b); therefore, 80% of the back-calculated CL_{int} was assigned to CYP3A4-mediated CL_{int} (194 μL/min/mg protein) with the remaining 20% as additional CL_{int} (49 μL/min/mg protein). The steady-state volume of distribution (V_{ss}) of crizotinib was predicted using the mathematical model 2 (Rodgers et al., 2005) implemented in Simcyp. To improve goodness-of-fit between predicted and observed plasma concentration-time profiles, crizotinib pK_a values were adjusted from 5.4 and 8.9 (diprotic base) to 7.6 (monoprotic base) to predict the clinically observed V_{ss} of 25 L/kg from the single intravenous infusion study (FDA, 2011). Using the unadjusted pK_a values of 5.4 and 8.9, the predicted crizotinib V_{ss} was 7.0 L/kg, which resulted in poor fits to the clinically observed single-dose intravenous infusion and oral plasma concentration profiles. Although a minimal-PBPK model implemented Simcyp reasonably predicted the areas under the plasma concentration-time curve (AUC), the maximum plasma concentration (C_{max}) was significantly under-predicted in both the single-dose intravenous infusion and oral plasma concentration profiles. Simulations for midazolam plasma concentration-time profiles were also performed by a full-PBPK model using a modified Simcyp-default midazolam file with the adjusted k_a of 2 h^{-1} and pK_a values of 7.4 (ampholyte). Mathematical model 2 implemented in Simcyp was used to predict midazolam V_{ss}. These adjustments were required to simulate comparable midazolam plasma concentration-time profiles to the clinically observed results in patients (n = 14) after a single oral administration of midazolam without co-administration of crizotinib (FDA, 2011). In addition to these adjustments, the predicted

Downloaded from dmd.aspetjournals.org at ASPET Journals on February 7, 2023

DMD Fast Forward. Published on November 5, 2012 as DOI: 10.1124/dmd.112.049114
This article has not been copyedited and formatted. The final version may differ from this version.

liver to plasma partition coefficients (k_p) were set to unity from 22 and 1.3 for crizotinib and midazolam, respectively. These changes resulted in minimal effects on the predicted V_{ss} values for both crizotinib (from 25.3 to 24.8 L/kg) and midazolam (from 1.0 to 1.1 L/kg).

Clinical trial simulation in Simcyp was performed with a virtual population of healthy volunteers in 8 trials of 10 subjects, each aged 18 to 65 years with a female/male ratio of 0.34, whose CYP3A4 degradation rate constant (k_{deg}) was 0.019 h^{-1} in the liver and 0.030 h^{-1} in the gastro-intestinal (GI) tract. The output sampling interval in Simcyp simulation tool box was set to 0.2 hours in all simulations. Trial designs used were as follows:

Trial #1: A single oral dose of crizotinib 250 mg was administered on day 1; crizotinib plasma concentration was simulated for 7 days.

Trial #2: Multiple doses of crizotinib, 250 mg twice daily with an interval of 12 hours, were orally administered for 28 days; crizotinib plasma concentration was simulated during crizotinib repeated administration.

Trial #3: A single oral dose of midazolam 2 mg was co-administered on day 28 with repeated oral doses of crizotinib (250 mg twice daily with an interval of 12 hours) for 28 days; plasma concentrations of midazolam and crizotinib were simulated during crizotinib repeated administration.

In these simulations, C_{max}, t_{max} and $AUC_{0-\tau}$ were obtained from Simcyp output whereas $AUC_{0-\infty}$ was calculated from simulated plasma concentrations using the linear trapezoidal rule:

$$AUC_{0-\infty} = AUC_{0-L} + C_L / \lambda \quad (5)$$

Downloaded from dmd.aspetjournals.org at ASPET Journals on February 7, 2023

DMD Fast Forward. Published on November 5, 2012 as DOI: 10.1124/dmd.112.049114
This article has not been copyedited and formatted. The final version may differ from this version.

where $AUC_{0\text{-}L}$, C_L and λ represent the area under the plasma concentration-time curve from time zero to the last time point, the plasma concentration at the last time point and the elimination rate constant in the terminal phase of log plasma concentration-time curves determined by linear regression, respectively.

Geometric means of PK parameters in 8 simulation trials were compared to the clinically observed geometric mean in order to assess Simcyp prediction accuracy. In addition to the Simcyp outputs of 5th and 95th percentiles of all 80 subjects, the geometric mean values of 5th and 95th percentiles among 8 simulation trials were calculated by Microsoft Excel 2007 (Microsoft, Redmond, WA) to compare to the clinically observed 5th and 95th percentiles in the crizotinib-midazolam interaction study.

Sensitivity Analysis for Crizotinib Hepatic k_p and CYP3A4 k_{deg} with Simcyp

The sensitivity analyses for crizotinib hepatic k_p value ranging from 1 to 24 and hepatic CYP3A4 k_{deg} from 0.693 to 0.00693 h^{-1} (i.e., $t_{1/2}$ of 1 to 100 hours) were separately performed in the prediction of crizotinib-midazolam interaction with Simcyp using CRZ-HSP. Clinical trial simulation in Simcyp was the same as trial #3 as described above, and the PK parameters (e.g., C_{max}, t_{max}, $AUC_{0\text{-}\tau}$ and $AUC_{0\text{-}\infty}$) and geometric mean values of 5th and 95th percentiles among 8 simulation trials were either obtained or calculated from Simcyp outputs as described above.

Prediction of Crizotinib-Midazolam Interaction with a Static Mathematical Model

A static mathematical model (Fahmi et al., 2008) was used to predict the fold-increase in midazolam $AUC_{0\text{-}\infty}$ (AUC_R) following co-administration with crizotinib:

Downloaded from dmd.aspetjournals.org at ASPET Journals on February 7, 2023

DMD Fast Forward. Published on November 5, 2012 as DOI: 10.1124/dmd.112.049114
This article has not been copyedited and formatted. The final version may differ from this version.

$$AUC_R = \left(\frac{1}{[A_h \times B_h \times C_h] \times f_m + (1 - f_m)} \right) \times \left(\frac{1}{[A_g \times B_g \times C_g] \times (1 - F_g) + F_g} \right) \quad (6)$$

$$A = \frac{k_{deg}}{k_{deg} + \frac{[I] \cdot k_{inact}}{[I] + K_I}} \quad (7)$$

$$B = 1 + \frac{d \cdot E_{max} \cdot [I]}{[I] + EC_{50}} \quad (8)$$

$$C = \frac{1}{1 + [I]/K_i} \quad (9)$$

where A, B and C represent TDI, EI and RI, respectively, and the subscripts *h* and *g* denote liver and GI tract, respectively.

Crizotinib input parameters and CYP3A4 k_{deg} values in the liver and GI tract used for the static model were exactly the same as Simcyp input parameters in order to compare in vivo DDI predictions between the dynamic and static models. Therefore, the proposed empirical scaling factor for induction (i.e., *d*) in the static model was set to unity since the EI parameters were already normalized with rifampin data for the dynamic model.

The availability in the GI tract (F_g) and $f_{m,CYP3A4}$ for midazolam were set as 0.63 and 0.93, respectively (Ernest et al., 2005; Obach et al., 2006). Crizotinib steady-state unbound average plasma concentrations ($C_{ave,u}$), that was calculated from $AUC_{0\text{-}\tau}$ divided by the dosing interval of 12 hours followed by the correction for $f_{u,plasma}$, was used as the hepatic inhibitor concentrations ($[I]_h$) in the static model (as consistent with a full-PBPK model with hepatic k_p of unity). The intestinal inhibitor concentrations ($[I]_g$) were calculated from crizotinib parameters summarized in Table 1 using the following equation (Rostami-Hodjegan and Tucker, 2004):

Downloaded from dmd.aspetjournals.org at ASPET Journals on February 7, 2023

DMD Fast Forward. Published on November 5, 2012 as DOI: 10.1124/dmd.112.049114
This article has not been copyedited and formatted. The final version may differ from this version.

$$[I]_g = D \cdot k_a \cdot F_a \cdot f_{u,gut} / Q_{gut} \quad (10)$$

where D, k_a, F_a, $f_{u,gut}$ and Q_{gut} represent the dose amount per dose (μmol), the first-order absorption rate constant (h^{-1}), the fraction of dose absorbed, the unbound fraction in the GI tract and the enterocyte blood flow (L/h), respectively.

Downloaded from dmd.aspetjournals.org at ASPET Journals on February 7, 2023

DMD Fast Forward. Published on November 5, 2012 as DOI: 10.1124/dmd.112.049114
This article has not been copyedited and formatted. The final version may differ from this version.

RESULTS

In vitro Effects of Crizotinib on CYP3A

Crizotinib TDI kinetic parameters for CYP3A were determined in HLM and HSP using midazolam as a CYP3A probe substrate. Estimated $K_{I,app}$ and k_{inact} in HLM were 3.0 μM and 6.9 h^{-1}, respectively (Fig. 2). Crizotinib IC_{50} curves in HSP were adequately described by the irreversible model (eq. 3) with $K_{I,app}$ of 9.6 μM and k_{inact} of 0.78 h^{-1} (Fig. 3). The estimates for K_I in HLM and HSP following the correction for in vitro non-specific binding (e.g., $f_{u,mic}$ and $f_{u,plasma}$, respectively) were 0.37 and 0.89 μM, respectively. Thus, the K_I value in HSP was approximately 3-fold higher than that in HLM whereas the k_{inact} from HSP was approximately 9-fold lower than that from HLM, resulting in the 20-fold difference in the inactivation efficiency (k_{inact} / K_I) between HLM and HSP (19 and 0.87 $h^{-1}\cdot\mu M^{-1}$, respectively). These K_I and k_{inact} values were used for Simcyp simulation (Table 1).

In cryopreserved HEP from three donors, crizotinib concentration-dependently induced CYP3A4 mRNA expression with estimated E_{max} of 6.4 to 29-fold and EC_{50} of 0.47 to 3.1 μM. It should be noted that relatively low cell viability (<0.7 ratio to vehicle control sample) was observed at higher crizotinib concentrations (≥5 μM); thus, the accuracy of EI parameter estimation might have been impacted. Following the normalization with rifampin data (positive control), mean crizotinib E_{max} of 2.4-fold and EC_{50} of 0.84 μM were used for Simcyp simulation (Table 1).

Predicted Crizotinib Plasma Concentrations with Simcyp

Clinically observed crizotinib C_{max}, t_{max} and $AUC_{0-\infty}$ were 87 ng/mL, 4 hours and 1817 ng·h/mL, respectively, in cancer patients (n = 8) after a single oral administration of

Downloaded from dmd.aspetjournals.org at ASPET Journals on February 7, 2023

DMD Fast Forward. Published on November 5, 2012 as DOI: 10.1124/dmd.112.049114
This article has not been copyedited and formatted. The final version may differ from this version.

crizotinib 250 mg (FDA, 2011). By the Simcyp simulation with CRZ-HLM, the predicted C_{max} (89 ng/mL) was within 10% of the observed value whereas the $AUC_{0-\infty}$ (3901 ng·h/mL) was over-predicted by 2.1-fold (Table 2). As shown in Fig. 4A, the predicted crizotinib plasma concentrations were slightly but consistently higher than the observed concentrations after t_{max}. In contrast, the predicted $AUC_{0-\infty}$ (1745 ng·h/mL) by Simcyp with CRZ-HSP was consistent with the observed value (<10%) whereas the predicted C_{max} (42 ng/mL) was under-predicted by approximately 2-fold (Table 2). It remained unclear why the C_{max} was under-predicted. One of the possible reasons could be the effect of multidrug-resistance transport protein, P-glycoprotein, on the absorption since crizotinib was reported to be a substrate of P-glycoprotein (FDA, 2011). The predicted crizotinib plasma concentrations with CRZ-HSP were in good agreement with the observed profiles after t_{max} (Fig. 4B).

Clinically observed crizotinib steady-state C_{max}, t_{max} and $AUC_{0-\tau}$ were 328 ng/mL, 4 hours and 3054 ng·h/mL, respectively, in cancer patients (n =5) after 28-day repeated oral administration of crizotinib 250 mg twice daily (FDA, 2011). The predicted C_{max} (543 ng/mL) and $AUC_{0-\tau}$ (6494 ng·h/mL) by Simcyp with CRZ-HLM were over-predicted by 1.7- and 2.1-fold, respectively (Table 2 and Fig. 4C). In contrast, the Simcyp-predicted crizotinib steady-state plasma concentrations with CRZ-HSP were in good agreement with the observed concentrations (Fig. 4D). The predicted C_{max} (273 ng/mL) and $AUC_{0-\tau}$ (3258 ng·h/mL) were within 20% of the observed values (Table 2). Additionally, the effect of crizotinib TDI or EI on crizotinib steady-state plasma concentrations was examined in a virtual population of healthy volunteers by Simcyp using CRZ-HSP with/without TDI and/or EI parameters. The predicted C_{max}

Downloaded from dmd.aspetjournals.org at ASPET Journals on February 7, 2023

DMD Fast Forward. Published on November 5, 2012 as DOI: 10.1124/dmd.112.049114
This article has not been copyedited and formatted. The final version may differ from this version.

(288 ng/mL) and $AUC_{0-\tau}$ (3432 ng·h/mL) with only TDI parameters were comparable to the predicted values (273 ng/mL and 3258 ng·h/mL, respectively) with both TDI and EI parameters (within 5%) whereas those with only EI parameters (128 ng/mL and 1519 ng·h/mL, respectively) were comparable to the predicted values (133 ng/mL and 1587 ng·h/mL, respectively) without TDI and EI parameters (within 5%). The predicted C_{max} and $AUC_{0-\tau}$ with only TDI parameters were approximately 2-fold higher than the predicted values without TDI and EI parameters. Based on these comparisons, crizotinib steady-state plasma concentrations appeared to be accumulated by 2-fold due to TDI with a minimal EI effect.

Predicted Crizotinib-Midazolam Interaction with Simcyp

Clinically observed midazolam C_{max}, t_{max} and $AUC_{0-\infty}$ in cancer patients (n = 14) after a single oral administration of midazolam 2 mg were reported to be 13 ng/mL, 0.5 hours and 32 ng·h/mL, respectively, without co-administration of crizotinib (FDA, 2011). After 28-day oral administration of twice daily doses of crizotinib 250 mg in cancer patients (n = 8), midazolam C_{max} and $AUC_{0-\infty}$ increased to 26 ng/mL and 117 ng·h/mL, respectively. Thus, the fold-increase in midazolam C_{max} (C_{maxR}) and AUC_R with co-administration of crizotinib were 2.0 and 3.7, respectively, suggesting crizotinib was a moderate CYP3A inhibitor (FDA, 2012). The 90% confidence intervals (*CI*) were 1.4 to 2.9 for C_{maxR} and 2.6 to 5.1 for AUC_R. When the crizotinib-midazolam interaction was predicted by Simcyp with CRZ-HLM, the predicted midazolam plasma concentration-time profiles were much higher than the observed profiles (Fig. 5A). The midazolam C_{maxR} and AUC_R were 3.0 and 21, respectively (Table 3 and Fig. 6A), resulting in the 1.5- and 5.6-fold over-predictions of C_{maxR} and AUC_R, respectively. In

Downloaded from dmd.aspetjournals.org at ASPET Journals on February 7, 2023

DMD Fast Forward. Published on November 5, 2012 as DOI: 10.1124/dmd.112.049114
This article has not been copyedited and formatted. The final version may differ from this version.

contrast, the predicted midazolam plasma concentration-time profiles with CRZ-HSP were relatively consistent with the observed profiles (Fig. 5B). The midazolam C_{maxR} and AUC_R (1.9 and 3.6, respectively) were in good agreement with the clinically observed results (Table 3 and Fig. 6B). The 90% *CI* for predicted C_{max} (1.4 to 2.9) was relatively consistent with the observed *CI*, whereas that for predicted $AUC_{0-\infty}$ (1.6 to 8.8) was slightly larger than the observed result.

Sensitivity Analysis for Crizotinib Hepatic k_p and CYP3A4 k_{deg} with Simcyp

The sensitivity analysis for crizotinib hepatic k_p values of 1 to 24 revealed that the midazolam AUC_R with co-administration of crizotinib varied markedly from 3.6 to 13, while the predicted crizotinib $AUC_{0-\tau}$ values were within 2-fold (3258 to 5434 ng·h/mL) (see Supplemental Data, Figure S1). Therefore, DDI prediction with a full-PBPK model in Simcyp was highly sensitive to crizotinib hepatic k_p value even though the PBPK model was basically constructed with perfusion-limited compartments in the absence of any diffusion barrier.

In the sensitivity analysis for hepatic CYP3A4 k_{deg} values of 0.693 to 0.00693 h^{-1} (i.e., $t_{1/2}$ of 1 to 100 hours), the predicted crizotinib steady-state C_{max} and C_{ave} varied from 141 to 385 ng/mL and 140 to 383 ng/mL, respectively, indicating that the CYP3A4 $t_{1/2}$ of 25 to 35 hours yielded the best prediction for crizotinib C_{ave} (Supplemental Data, Figure S2). The midazolam C_{maxR} and AUC_R varied from 1.3 to 2.4 and 1.3 to 7.7, respectively. Thus, the AUC_R was more sensitive to the hepatic k_{deg} values relative to C_{maxR}. The $t_{1/2}$ of 30 to 40 hours yielded the best prediction of the midazolam AUC_R. Therefore, the hepatic k_{deg} value of 0.019 h^{-1} ($t_{1/2}$ of 36 hours) used in this study was

Downloaded from dmd.aspetjournals.org at ASPET Journals on February 7, 2023

DMD Fast Forward. Published on November 5, 2012 as DOI: 10.1124/dmd.112.049114
This article has not been copyedited and formatted. The final version may differ from this version.

within a range of reasonable predictions on both the crizotinib steady-state plasma concentrations and crizotinib-midazolam interaction.

Predicted Crizotinib-Midazolam Interaction by Static Models

The predicted midazolam AUC_R values with the static mathematical model using either clinically observed or Simcyp-predicted crizotinib $C_{ave,u}$ are summarized in Table 4. Using the clinically observed crizotinib $C_{ave,u}$, the predicted midazolam AUC_R values with HLM-TDI and HSP-TDI were 17 and 3.2, respectively. Thus, the midazolam AUC_R with HLM-TDI was over-predicted by approximately 5-fold whereas the prediction with HSP-TDI was consistent with the observed AUC_R. In the static model, the midazolam AUC_R in the liver (11 to 12) with HLM-TDI was much higher than that with HSP-TDI (2.5 to 2.6), whereas the AUC_R in the intestines was relatively comparable between HLM-TDI and HSP-TDI (1.6 and 1.3, respectively). This comparable intestinal AUC_R between HLM-TDI and HSP-TDI appeared to be largely due to midazoalm F_g of 0.63, which resulted in the maximal effect of 1.6-fold increase. Using the Simcyp-predicted crizotinib $C_{ave,u}$ by HLM-TDI and HSP-TDI, the predicted midazolam AUC_R values were 19 and 3.3, respectively. Thus, the prediction results of crizotinib–midazolam interaction with the static model using the Simcyp-predicted crizotinib $C_{ave,u}$ were relatively consistent with those with the Simcyp full-PBPK models with k_p of unity.

In addition, the predicted midazolam AUC_R values with Simcyp static model (R_{ss}) were 13 and 2.3 with HLM-TDI and HSP-TDI, respectively. These AUC_R values were approximately 1.5-fold lower than the predicted values with the Simcyp full-PBPK models (i.e., 21 and 3.6, respectively). The difference in the predicted ratios between the R_{ss} and full-PBPK predictions appeared to be largely due to the crizotinib TDI effects on

Downloaded from dmd.aspetjournals.org at ASPET Journals on February 7, 2023

DMD Fast Forward. Published on November 5, 2012 as DOI: 10.1124/dmd.112.049114
This article has not been copyedited and formatted. The final version may differ from this version.

the accumulation of crizotinib steady-state plasma concentrations, which was not taken into account for the Simcyp-R_{ss} prediction, where the inhibitor concentration was calculated from the input PK parameters such as *D* and *CL*.

Downloaded from dmd.aspetjournals.org at ASPET Journals on February 7, 2023

DMD Fast Forward. Published on November 5, 2012 as DOI: 10.1124/dmd.112.049114
This article has not been copyedited and formatted. The final version may differ from this version.

DISCUSSION

In the present study, the estimated in vitro inactivation efficiency (k_{inact} / K_I) for crizotinib TDI potency was approximately 20-fold lower in HSP relative to HLM. Consistent with the present results, the known CYP3A inhibitors (e.g., diltiazem, erythromycin and verapamil) were also reported to be less potent in HEP compared to HLM, and the difference in TDI potency have yielded an impact on in vivo DDI prediction (Xu et al., 2009; Chen et al., 2011). The advantages in utilization of HEP over HLM are considered to be that HEP are intact cellular systems containing not only a full complement of phase I/II metabolizing enzymes but also functional cell membranes. The estimated k_{inact} in HEP is generally considered an apparent hybrid kinetic parameter consisting of 1) the rate of diffusion through the cell membrane, 2) the total metabolic consumption rate (including sequential metabolism), and 3) the intrinsic enzyme inactivation rate. Therefore, these factors could be important for some drugs showing substantially different intra- versus extracellular concentrations and/or multiple metabolic pathways, particularly those associated with non-CYPs (Zhao, 2008). Crizotinib was primarily metabolized by CYP3A (Johnson et al., 2011a), and its passive permeability was relatively low (approximately 1×10^{-6} cm/sec) in the recently reported permeability assay system using low-efflux Madin-Darby canine kidney cells (Di et al., 2011). Crizotinib was also reported to be a substrate of P-glycoprotein as mentioned above. Thus, these factors could potentially lead to differences in intra- versus extracellular concentrations, and, correspondingly, to differences in the estimated TDI potency between HLM versus HSP.

Downloaded from dmd.aspetjournals.org at ASPET Journals on February 7, 2023

DMD Fast Forward. Published on November 5, 2012 as DOI: 10.1124/dmd.112.049114
This article has not been copyedited and formatted. The final version may differ from this version.

Mathematical models used in the Simcyp-PBPK model are the well-stirred and "Q_{gut}" models in the liver and GI tract, respectively (Yang et al., 2007; Jamei et al., 2009). The well-stirred model assumes that drug distribution into liver is perfusion-limited without any diffusion delay; therefore, unbound drug concentration within liver is in equilibrium with unbound drug concentration in liver outlet, e.g., $C_{sys,u}$. Accordingly, we intended to use crizotinib $C_{sys,u}$ as the inhibitor concentration for DDI prediction by adjusting hepatic k_p value (i.e., unity) as described in Materials and Methods. Consistent with our findings, other investigators (Obach et al., 2007; Fahmi et al., 2009; Boulenc and Barberan, 2011) reported that the use of $C_{sys,u}$ (e.g., $C_{max,u}$ or $C_{ave,u}$) as the inhibitor concentrations yielded the most accurate DDI predictions for TDI and EI by the static models. When the projected/calculated $C_{inlet,u}$ was used, the DDI predictions for TDI and EI were generally over-predicted while those for RI were more accurately predicted. These findings may suggest that RI mainly occurs during the first-pass metabolism process, whereas TDI and EI continue to take place beyond the first-pass metabolism. Consistently, the clinically observed crizotinib-midazolam interaction was more significant on midazolam AUC_R than C_{maxR}, and the DDI prediction using crizotinib $C_{sys,u}$ yielded a reasonable prediction for both midazolam AUC_R and C_{maxR}. Thus, crizotinib $C_{sys,u}$ appears to be a more appropriate inhibitor concentration than $C_{inlet,u}$ for the prediction of crizotinib-midazolam interaction.

The Q_{gut} model in the GI tract is basically constructed by the well-stirred model, where the blood flow term (i.e., Q_{gut}) is a hybrid parameter consisting of a compound-dependent permeability through enterocyte membrane and a physiological villous blood flow. Crizotinib Q_{gut} value was estimated to be 4 L/h based on a calculated $P_{eff,man}$ value

Downloaded from dmd.aspetjournals.org at ASPET Journals on February 7, 2023

DMD Fast Forward. Published on November 5, 2012 as DOI: 10.1124/dmd.112.049114
This article has not been copyedited and formatted. The final version may differ from this version.

of 0.58×10^{-4} cm/s derived from its physicochemical properties. This $P_{eff,man}$ value was within a moderate range among seventeen compounds reported (Yang et al., 2007). Since crizotinib F_g was estimated to be approximately 0.9 by the Q_{gut} model, its moderate $P_{eff,man}$ did not appear to be a limiting factor for the first-pass metabolism in the GI tract. In contrast, the experimentally measured crizotinib in vitro permeability (1×10^{-6} cm/sec) seemed to be lower than the value expected from its physicochemical properties, suggesting that the calculated $P_{eff,man}$ value might be over-predicted. However, crizotinib permeability can be taken into account to estimate TDI kinetic parameters in HSP because this system contains intact cell membranes. We therefore believe that a perfusion-limited model is appropriate for PK and/or DDI prediction when the kinetic parameters were determined in an in vitro system containing cell membranes. On the other hand, a diffusion rate through the cell membrane would likely be an important factor for PBPK model of low permeable compounds when their kinetic parameters were determined in assay systems without functional cell membranes (e.g., HLM). In such a case, a diffusion-limited model would be likely required for their PK and/or DDI prediction. Moreover, when compounds are metabolized by multiple enzymes such as microsomal and cytosolic enzymes, HEP would be more appropriate to determine TDI kinetic parameters by taking into account of an overall in vivo metabolic pathway. It has been reported that multiple enzymes (e.g., CYP3A and aldehyde oxidase) were involved in the crizotinib metabolism (Johnson et al., 2011a); therefore, this might be another factor that contributed to the difference in the TDI kinetics between HLM and HSP. These considerations are graphically summarized in Fig. 7. For PBPK model-based DDI prediction, the selection of either a perfusion- or diffusion-limited model should be

Downloaded from dmd.aspetjournals.org at ASPET Journals on February 7, 2023

DMD Fast Forward. Published on November 5, 2012 as DOI: 10.1124/dmd.112.049114
This article has not been copyedited and formatted. The final version may differ from this version.

carefully considered based upon each inhibitor's property and in vitro assay system used. It should also be important to select/simulate appropriate surrogate concentrations of both object and precipitant drugs as the unbound concentrations at target sites. In vivo DDI predictions are expected to be more accurate based on plasma concentration-profiles predicted by the PBPK model compared to a fixed inhibitor concentration (e.g., $C_{max,u}$ and $C_{ave,u}$) used for the static model. In the prediction of crizotinib-midazolam interaction, it would be worth noting that the Simcyp minimal- and full-PBPK models (with hepatic k_p of unity) yielded comparable DDI predictions when the predicted crizotinib concentrations in plasma were comparable between these models (Supplemental Data, Table S1). Moreover, these DDI predictions were roughly comparable to the predictions from the static models such as a Simcyp-static model (i.e., R_{ss}) and a static mathematical model (Supplemental Data, Table S1). Therefore, there might not be significant differences in DDI prediction between dynamic and static models if the factors related to DDI were appropriately incorporated into these models. However, these comparable predictions for crizotinib-midazolam interaction could be largely due to the relatively flat crizotinib plasma concentration time-profiles (i.e., $C_{max} \approx C_{ave}$) during dosing interval as shown in Fig 4.

Several other factors related to TDI mechanism should also be considered for the in vivo DDI prediction. Quantitative measurement of in vivo CYP3A4 k_{deg} in humans remains a challenge as k_{deg} is often associated with an uncertainty in the DDI prediction (Obach et al., 2007; Rowland Yeo et al., 2011). Not surprisingly, a wide range of hepatic k_{deg} values has been reported for CYP3A4 as turnover half-lives ($t_{1/2}$) of 10 to 140 h (Yang et al., 2008; Grimm et al., 2009; Xu et al., 2009; Chen et al., 2011). We used the

Downloaded from dmd.aspetjournals.org at ASPET Journals on February 7, 2023

DMD Fast Forward. Published on November 5, 2012 as DOI: 10.1124/dmd.112.049114
This article has not been copyedited and formatted. The final version may differ from this version.

Simcyp default k_{deg} values of 0.019 h^{-1} ($t_{1/2}$ = 36 hours) in the liver and 0.030 h^{-1} ($t_{1/2}$ = 23 hours) in the intestines. Based on the sensitivity analysis for hepatic CYP3A4 k_{deg} values ranging from 0.693 to 0.00693 h^{-1}, i.e., $t_{1/2}$ of 1 to 100 hours, the hepatic k_{deg} value of 0.019 h^{-1} ($t_{1/2}$ of 36 hours) used in this study was within a range of reasonable predictions on both the crizotinib steady-state plasma concentrations and crizotinib-midazolam interaction (Supplemental Data, Figure S2). Another important parameter is the fraction metabolized by a drug-metabolizing enzyme, e.g., $f_{m,CYP3A4}$. The estimated crizotinib $f_{m,CYP3A4}$ was approximately 0.8 based on the in vitro CYP phenotyping study and the human mass-balance study with [^{14}C]crizotinib (Johnson et al., 2011a; Johnson et al., 2011b); the $f_{m,CYP3A4}$ of 0.8 used in the present study yielded reasonable PK/DDI predictions.

Despite these reasonable DDI predictions, the method used in the present study included potential limitations that should be addressed. First, neither in vitro non-specific binding nor any decrease in crizotinib concentration during incubation was considered for the correction of in vitro crizotinib EI parameters (e.g., E_{max} and EC_{50}), as previously reported (Fahmi et al., 2008). In contrast, the obtained TDI parameters in HLM and HSP were corrected for the in vitro non-specific binding. Secondly, and possibly more importantly, the physiological CYP3A4 kinetic (or systems) parameters (i.e., k_{syn} and k_{deg}) for the TDI prediction were assumed to remain constant in the presence of inhibitor, and an additional enzyme degradation pathway was introduced to reach new steady-state concentration as k_{obs} (eq. 1). This assumption may not be valid when EI occurs in parallel to TDI. In fact, there appears to be limited understanding of underlying simultaneous in vitro-to-in vivo extrapolation for TDI and EI (and its possible interplay).

Downloaded from dmd.aspetjournals.org at ASPET Journals on February 7, 2023

DMD Fast Forward. Published on November 5, 2012 as DOI: 10.1124/dmd.112.049114
This article has not been copyedited and formatted. The final version may differ from this version.

Moreover, although TDI and EI of CYP3A are known to occur in both liver and GI tract, their magnitudes may be different in these organs. Despite these limitations, a PBPK modeling approach for DDI prediction affords an opportunity to gain greater insight into the underlying mechanisms mediating these complex interactions as a function of time with the effects of intrinsic factors such as organ dysfunction, age and genetics.

Downloaded from dmd.aspetjournals.org at ASPET Journals on February 7, 2023

DMD Fast Forward. Published on November 5, 2012 as DOI: 10.1124/dmd.112.049114
This article has not been copyedited and formatted. The final version may differ from this version.

Acknowledgment

We greatly acknowledge Sascha Freiwald and Danielle Smith (Pharmacokinetics, Dynamics and Metabolism (PDM), Pfizer, San Diego, CA) for the bioanalytical assay and Odette A. Fahmi and Sherri Boldt (PDM, Pfizer, Groton, CT) for the enzyme induction. We also thank Weiwei Tan and Keith D. Wilner (Clinical Pharmacology, Pfizer, San Diego, CA) for valuable discussion about clinical pharmacokinetic data, and Odette A. Fahmi (PDM, Pfizer, Groton, CT), R. Scott Obach (PDM, Pfizer, Groton, CT), Bill J. Smith (PDM, Pfizer, San Diego, CA) and Bhasker Shetty (PDM, Pfizer, San Diego, CA) for excellent inputs for the draft manuscript.

Downloaded from dmd.aspetjournals.org at ASPET Journals on February 7, 2023

DMD Fast Forward. Published on November 5, 2012 as DOI: 10.1124/dmd.112.049114
This article has not been copyedited and formatted. The final version may differ from this version.

Authorship Contribution

Participated in research design: Mao and Yamazaki

Conduct experiments: Mao, Shen and Yamazaki

Performed data analysis: Mao and Yamazaki

Wrote or contribute to the writing of the manuscript: Mao, Shen, Johnson and Yamazaki

Downloaded from dmd.aspetjournals.org at ASPET Journals on February 7, 2023

DMD Fast Forward. Published on November 5, 2012 as DOI: 10.1124/dmd.112.049114
This article has not been copyedited and formatted. The final version may differ from this version.

References

Boulenc X and Barberan O (2011) Metabolic-based drug-drug interactions prediction, recent approaches for risk assessment along drug development. *Drug Metabol Drug Interact* **26:**147-168.

Chen Y, Liu L, Monshouwer M and Fretland AJ (2011) Determination of time-dependent inactivation of CYP3A4 in cryopreserved human hepatocytes and assessment of human drug-drug interactions. *Drug Metab Dispos* **39:**2085-2092.

Chu V, Einolf HJ, Evers R, Kumar G, Moore D, Ripp S, Silva J, Sinha V, Sinz M and Skerjanec A (2009) In vitro and in vivo induction of cytochrome p450: a survey of the current practices and recommendations: a pharmaceutical research and manufacturers of america perspective. *Drug Metab Dispos* **37:**1339-1354.

Cui JJ, Tran-Dube M, Shen H, Nambu M, Kung PP, Pairish M, Jia L, Meng J, Funk L, Botrous I, McTigue M, Grodsky N, Ryan K, Padrique E, Alton G, Timofeevski S, Yamazaki S, Li Q, Zou H, Christensen J, Mroczkowski B, Bender S, Kania RS and Edwards MP (2011) Structure based drug design of crizotinib (PF-02341066), a potent and selective dual inhibitor of mesenchymal-epithelial transition factor (c-MET) kinase and anaplastic lymphoma kinase (ALK). *J Med Chem* **54:**6342-6363.

Di L, Keefer C, Scott DO, Strelevitz TJ, Chang G, Bi YA, Lai Y, Duckworth J, Fenner K, Troutman MD and Obach RS (2012) Mechanistic insights from comparing intrinsic clearance values between human liver microsomes and hepatocytes to guide drug design. *Eur J Med Chem***:**doi.10.1016/j.ejmech.2012.1006.1043.

Di L, Whitney-Pickett C, Umland JP, Zhang H, Zhang X, Gebhard DF, Lai Y, Federico JJ, 3rd, Davidson RE, Smith R, Reyner EL, Lee C, Feng B, Rotter C, Varma MV, Kempshall S, Fenner K, El-Kattan AF, Liston TE and Troutman MD (2011) Development of a new permeability assay using low-efflux MDCKII cells. *J Pharm Sci* **100:**4974-4985.

Ernest CS, 2nd, Hall SD and Jones DR (2005) Mechanism-based inactivation of CYP3A by HIV protease inhibitors. *J Pharmacol Exp Ther* **312:**583-591.

Fahmi OA, Maurer TS, Kish M, Cardenas E, Boldt S and Nettleton D (2008) A combined model for predicting CYP3A4 clinical net drug-drug interaction based on CYP3A4 inhibition, inactivation, and induction determined in vitro. *Drug Metab Dispos* **36:**1698-1708.

Fahmi OA, Hurst S, Plowchalk D, Cook J, Guo F, Youdim K, Dickins M, Phipps A, Darekar A, Hyland R and Obach RS (2009) Comparison of different algorithms for predicting clinical drug-drug interactions, based on the use of CYP3A4 in vitro data: predictions of compounds as precipitants of interaction. *Drug Metab Dispos* **37:**1658-1666.

FDA (2011) Xalkori Clinical Pharmacology and Biopharmaceutical Review(s) (http://www.accessdata.fda.gov/drugsatfda_docs/nda/2011/202570Orig1s000ClinPharmR.pdf).

FDA (2012) Drug Interaction Studies — Study Design, Data Analysis, Implications for Dosing, and Labeling Recommendations (http://www.fda.gov/downloads/Drugs/GuidanceComplianceRegulatoryInformation/Guidances/ucm292362.pdf).

Downloaded from dmd.aspetjournals.org at ASPET Journals on February 7, 2023

DMD Fast Forward. Published on November 5, 2012 as DOI: 10.1124/dmd.112.049114
This article has not been copyedited and formatted. The final version may differ from this version.

Grimm SW, Einolf HJ, Hall SD, He K, Lim HK, Ling KH, Lu C, Nomeir AA, Seibert E, Skordos KW, Tonn GR, Van Horn R, Wang RW, Wong YN, Yang TJ and Obach RS (2009) The conduct of in vitro studies to address time-dependent inhibition of drug-metabolizing enzymes: a perspective of the pharmaceutical research and manufacturers of America. *Drug Metab Dispos* **37:**1355-1370.

Jamei M, Marciniak S, Feng K, Barnett A, Tucker G and Rostami-Hodjegan A (2009) The Simcyp population-based ADME simulator. *Expert Opin Drug Metab Toxicol* **5:**211-223.

Johnson TR, Zhou S, Lee C, Clouser-Roche A, Freiwald S, Youdim KA, Aherne K, Batugo MR, Skaptason J, Yamazaki S, Wester MR and Smith BJ (2011a) Identification of the human enzymes invovlved in the oxidative metabolism of crizotinib. *at the 17th North American Regional ISSX Meeting; 2011 Oct 16–20; Atlanta, GA. International Society for the Study of Xenobiotics, Washington, DC.*

Johnson TR, Goulet L, Smith EB, Yamazaki S, Walker GS, Tan W, Li C, Ni Y, Bedarida G, Brega N, Dalvie D and Smith BJ (2011b) Metabolism, excretion and pharmacokinetics of [^{14}C]crizotinib following oral administration to healthy subjects. *at the 17th North American Regional ISSX Meeting; 2011 Oct 16–20; Atlanta, GA. International Society for the Study of Xenobiotics, Washington, DC.*

Jones HM, Parrott N, Jorga K and Lave T (2006) A novel strategy for physiologically based predictions of human pharmacokinetics. *Clin Pharmacokinet* **45:**511-542.

Kanamitsu S, Ito K, Green CE, Tyson CA, Shimada N and Sugiyama Y (2000) Prediction of in vivo interaction between triazolam and erythromycin based on in vitro studies using human liver microsomes and recombinant human CYP3A4. *Pharm Res* **17:**419-426.

Kirby BJ, Collier AC, Kharasch ED, Whittington D, Thummel KE and Unadkat JD (2011) Complex drug interactions of HIV protease inhibitors 1: inactivation, induction, and inhibition of cytochrome P450 3A by ritonavir or nelfinavir. *Drug Metab Dispos* **39:**1070-1078.

Lave T, Parrott N, Grimm HP, Fleury A and Reddy M (2007) Challenges and opportunities with modelling and simulation in drug discovery and drug development. *Xenobiotica* **37:**1295-1310.

Mao J, Mohutsky MA, Harrelson JP, Wrighton SA and Hall SD (2011) Prediction of CYP3A-mediated drug-drug interactions using human hepatocytes suspended in human plasma. *Drug Metab Dispos* **39:**591-602.

Mao J, Mohutsky M, Harrelson J, Wrighton S and Hall S (2012) Predictions of CYP-Mediated Drug-Drug Interactions Using Cryopreserved Human Hepatocytes: Comparison of Plasma and Protein-Free Media Incubation Conditions. *Drug Metab Dispos* **40:**706-716.

Mayhew BS, Jones DR and Hall SD (2000) An in vitro model for predicting in vivo inhibition of cytochrome P450 3A4 by metabolic intermediate complex formation. *Drug Metab Dispos* **28:**1031-1037.

Nestorov I (2007) Whole-body physiologically based pharmacokinetic models. *Expert Opin Drug Metab Toxicol* **3:**235-249.

Obach RS, Walsky RL, Venkatakrishnan K, Gaman EA, Houston JB and Tremaine LM (2006) The utility of in vitro cytochrome P450 inhibition data in the prediction of drug-drug interactions. *J Pharmacol Exp Ther* **316:**336-348.

Downloaded from dmd.aspetjournals.org at ASPET Journals on February 7, 2023

DMD Fast Forward. Published on November 5, 2012 as DOI: 10.1124/dmd.112.049114
This article has not been copyedited and formatted. The final version may differ from this version.

Obach RS, Walsky RL and Venkatakrishnan K (2007) Mechanism-based inactivation of human cytochrome p450 enzymes and the prediction of drug-drug interactions. *Drug Metab Dispos* **35:**246-255.

Rodgers T, Leahy D and Rowland M (2005) Physiologically based pharmacokinetic modeling 1: predicting the tissue distribution of moderate-to-strong bases. *J Pharm Sci* **94:**1259-1276.

Rostami-Hodjegan A and Tucker G (2004) 'In silico' simulations to assess the 'in vivo' consequences of 'in vitro' metabolic drug–drug interactions. *Drug Discovery Today* **1:**441–448.

Rowland Yeo K, Walsky RL, Jamei M, Rostami-Hodjegan A and Tucker GT (2011) Prediction of time-dependent CYP3A4 drug-drug interactions by physiologically based pharmacokinetic modelling: impact of inactivation parameters and enzyme turnover. *Eur J Pharm Sci* **43:**160-173.

Shimada T, Yamazaki H, Mimura M, Inui Y and Guengerich FP (1994) Interindividual variations in human liver cytochrome P-450 enzymes involved in the oxidation of drugs, carcinogens and toxic chemicals: studies with liver microsomes of 30 Japanese and 30 Caucasians. *J Pharmacol Exp Ther* **270:**414-423.

Slaughter RL and Edwards DJ (1995) Recent advances: the cytochrome P450 enzymes. *Ann Pharmacother* **29:**619-624.

Xu L, Chen Y, Pan Y, Skiles GL and Shou M (2009) Prediction of human drug-drug interactions from time-dependent inactivation of CYP3A4 in primary hepatocytes using a population-based simulator. *Drug Metab Dispos* **37:**2330-2339.

Yamazaki S, Skaptason J, Romero D, Vekich S, Jones HM, Tan W, Wilner KD and Koudriakova T (2011) Prediction of oral pharmacokinetics of cMet kinase inhibitors in humans: physiologically based pharmacokinetic model versus traditional one-compartment model. *Drug Metab Dispos* **39:**383-393.

Yang J, Jamei M, Yeo KR, Tucker GT and Rostami-Hodjegan A (2007) Prediction of intestinal first-pass drug metabolism. *Curr Drug Metab* **8:**676-684.

Yang J, Liao M, Shou M, Jamei M, Yeo KR, Tucker GT and Rostami-Hodjegan A (2008) Cytochrome p450 turnover: regulation of synthesis and degradation, methods for determining rates, and implications for the prediction of drug interactions. *Curr Drug Metab* **9:**384-394.

Zhao P (2008) The use of hepatocytes in evaluating time-dependent inactivation of P450 in vivo. *Expert Opin Drug Metab Toxicol* **4:**151-164.

Zhao P, Kunze KL and Lee CA (2005) Evaluation of time-dependent inactivation of CYP3A in cryopreserved human hepatocytes. *Drug Metab Dispos* **33:**853-861.

Zimmerlin A, Trunzer M and Faller B (2011) CYP3A time-dependent inhibition risk assessment validated with 400 reference drugs. *Drug Metab Dispos* **39:**1039-1046.

Downloaded from dmd.aspetjournals.org at ASPET Journals on February 7, 2023

DMD Fast Forward. Published on November 5, 2012 as DOI: 10.1124/dmd.112.049114
This article has not been copyedited and formatted. The final version may differ from this version.

Footnotes

Send reprint requests to: Shinji Yamazaki, Ph.D., Pharmacokinetics, Dynamics and Metabolism, La Jolla Laboratories, Pfizer Worldwide Research and Development, 10777 Science Center Drive, San Diego, CA 92121.

E-mail: shinji.yamazaki@pfizer.com

Current affiliation (Jialin Mao): Department of Drug Metabolism & Pharmacokinetics, Genentech, A Member of the Roche Group, South San Francisco, CA.

Downloaded from dmd.aspetjournals.org at ASPET Journals on February 7, 2023

DMD Fast Forward. Published on November 5, 2012 as DOI: 10.1124/dmd.112.049114
This article has not been copyedited and formatted. The final version may differ from this version.

Legends for Figures

Fig. 1. Chemical structure of crizotinib

Fig. 2. Time-dependent inhibition by crizotinib for CYP3A in HLM. The x-axis represents crizotinib concentration in micromolars and the y-axis represents the observed apparent inactivation rate constant, k_{obs}, (●) and its fitting curve (—) in reciprocal hours. Data are the mean of duplicate determination.

Fig. 3. Time-dependent inhibition by crizotinib for CYP3A in HSP. The x-axis represents crizotinib concentration in micromolars on a logarithmic scale and the y-axis represents the ratio of remaining CYP3A enzyme activity to the vehicle control at the end of 35-minute incubation with midazolam following 0 (●), 10 (◆) or 20 (■)-minute preincubation with crizotinib alone. The dashed lines represent the best fitting curves for each incubation period by the irreversible model. Data are the mean of duplicate determination.

Downloaded from dmd.aspetjournals.org at ASPET Journals on February 7, 2023

DMD Fast Forward. Published on November 5, 2012 as DOI: 10.1124/dmd.112.049114
This article has not been copyedited and formatted. The final version may differ from this version.

Fig. 4. Observed and Simcyp-predicted plasma concentrations of crizotinib in patients after a single or 28-day repeated oral administration of crizotinib.

Crizotinib was orally administered at a single dose of 250 mg (n = 8) or multiple doses of 250 mg twice daily (n = 5) to cancer patients. The x-axis represents the time after a single (A and B) or 28-day repeated (C and D) oral administration of crizotinib in hours and the y-axis represents the observed (○) and Simcyp-predicted (—) plasma concentrations of crizotinib in nanograms per milliliter on a logarithmic scale using TDI parameters from HLM (A and C) or HSP (B and D). The observed and predicted plasma concentrations are expressed as mean ± SD and mean with 90% confidence interval (dashed line), respectively.

Fig. 5. Observed and Simcyp-predicted plasma concentrations of midazolam in patients before and after 28-day repeated oral administration of crizotinib.

Midazolam (2 mg) was orally administered to cancer patients before (n = 14) and after (n = 8) twice daily doses of crizotinib 250 mg for 28 days. The x-axis represents the time after a single oral administration of midazolam in hours and the y-axis represents the observed plasma concentrations of midazolam before (○) and after (●) oral administration of crizotinib in nanograms per milliliter on a logarithmic scale along with the predicted plasma concentrations before (---) and after (—) crizotinib administration by Simcyp with TDI parameters from HLM (A) or HSP (B). The observed and predicted plasma concentrations are expressed as mean ± SD and mean, respectively.

Downloaded from dmd.aspetjournals.org at ASPET Journals on February 7, 2023

DMD Fast Forward. Published on November 5, 2012 as DOI: 10.1124/dmd.112.049114
This article has not been copyedited and formatted. The final version may differ from this version.

Fig. 6. Clinically observed and Simcyp-predicted fold-increase in midazolam $AUC_{0-\infty}$ with co-administration of crizotinib. Midazolam (2 mg) was orally administered to cancer patients before (n = 14) and after (n = 8) twice daily doses of crizotinib 250 mg for 28 days. The x-axis represents the observed (Obs) and predicted 8 clinical trials (#1 to 8) of 10 individuals by Simcyp with TDI parameters from HLM (A) or HSP (B) and the y-axis represents the fold-increase in midazolam $AUC_{0-\infty}$ (AUC_R) with co-administration of crizotinib. The observed and predicted AUC_R values in each trial are expressed as geometric mean with 90% confidence interval. The solid and dashed lines represent geometric mean and 90% confidence interval, respectively, of all trials.

Fig.7. Proposed general scheme of PBPK model-based in vivo TDI prediction.

Downloaded from dmd.aspetjournals.org at ASPET Journals on February 7, 2023

TABLE 1

Physicochemical and pharmacokinetic parameters of crizotinib used for DDI prediction

Parameters (units)		Parameters (units)	
Molecular weight	450.34	CL_{int} *(μL/min/mg protein)*	
logP	4.29	$CL_{int,CYP3A4}$	194
pK_a [a]	5.4 & 8.9	$CL_{int,others}$	49
PSA (Å²)	78	Time-dependent inhibition on CYP3A in HLM	
$f_{u,plasma}$	0.093	K_I *(μM)*	0.37
R_{bp}	1.1	k_{inact} *(h^{-1})*	6.9
$f_{u,blood}$ [b]	0.085	Time-dependent inhibition on CYP3A in HSP	
$f_{u,mic}$	0.12	K_I *(μM)*	0.89
F_a	0.6	k_{inact} *(h^{-1})*	0.78
k_a *(h^{-1})* [c]	0.01 - 0.18	CYP3A4 induction in HEP [d]	
Q_{gut} *(L/h)*	4.0	E_{max} *(fold)*	2.4
$f_{u,gut}$	0.085	EC_{50} *(μM)*	0.84
V_{ss} *(L/kg)*	25	Reversible Inhibition on CYP3A4 in HLM	
		IC_{50} *(μM)*	>30

[a] The value of pk_a was adjusted from 5.4 and 8.9 (diprotic base) to 7.6 (monprotic base) to predict clinically observed V_{ss} of 25 L/kg.

[b] The value of $f_{u,blood}$ was calculated by $f_{u,plasma}$ and R_{bp}.

[c] The values of k_a were adjusted to simulate clinically observed t_{max} of approximately 4 hours in each simulation.

[d] The values of E_{max} and EC_{50} were determined in cryopreserved human hepatocytes from three donors (6.4 to 29-fold and 0.47 to 3.1 μM, respectively) followed by normalization with rifampin data (positive control)

Downloaded from dmd.aspetjournals.org at ASPET Journals on February 7, 2023

DMD Fast Forward. Published on November 5, 2012 as DOI: 10.1124/dmd.112.049114
This article has not been copyedited and formatted. The final version may differ from this version.

TABLE 2

Clinically observed and Simcyp-predicted pharmacokinetic parameter estimates of crizotinib in humans after a single or 28-day repeated oral administration of crizotinib.

	Single Dose (250 mg)		Repeated Doses (250 mg bid)	
	C_{max} *ng/mL*	$AUC_{0-\infty}$ *ng·h/mL*	C_{max} *ng/mL*	$AUC_{0-\tau}$ *ng·h/mL*
Observed	87 (34)	1817(33)	328 (25)	3054 (32)
Predicted				
HLM [a]	89 (43)	3901 (57)	543 (41)	6494 (41)
P/O ratio [b]	1.0	2.1	1.7	2.1
HSP [a]	42 (52)	1745 (72)	273 (64)	3258 (65)
P/O ratio [b]	0.48	0.96	0.83	1.1

Data are expressed as geometric mean (% coefficient of variation) for single dose (n = 8 patients) and 28-day repeated doses (n = 5 patients).

[a] Simcyp simulation was performed using TDI parameters from either HLM or HSP.

[b] Calculated mean ratio of predicted to observed pharmacokinetic parameters.

Downloaded from dmd.aspetjournals.org at ASPET Journals on February 7, 2023

DMD Fast Forward. Published on November 5, 2012 as DOI: 10.1124/dmd.112.049114
This article has not been copyedited and formatted. The final version may differ from this version.

TABLE 3

Clinically observed and Simcyp-predicted pharmacokinetic parameter estimates of midazolam in humans before and after 28-day repeated oral administration of crizotinib twice daily doses of 250 mg

	Crizotinib Administration	C_{max} *ng/mL*	$AUC_{0-\infty}$ *ng·h/mL*	Fold-increase in midazolam oral exposure [a]			
				C_{maxR}	90% CI	AUC_R	90% CI [a]
Observed	Pre	13 (39)	32 (41)				
	Post	26 (44)	117 (61)	2.0	1.4 - 2.9	3.7	2.6 - 5.1
Predicted	Pre	10 (58)	27 (90)				
P/O ratio [b]		0.77	0.83				
HLM [c]	Post	30 (39)	547 (70)	3.0	1.8 – 6.9	21	4.7 – 72
P/O ratio [b]		1.2	4.7	1.5		5.6	
HSP [c]	Post	19 (53)	97 (109)	1.9	1.4 - 2.7	3.6	1.6 – 8.8
P/O ratio [b]		0.72	0.83	0.94		1.0	

Data are expressed as geometric mean (% coefficient of variation) for pre- and post-doses of crizotinib (n = 14 and 8 patients, respectively).

[a] Fold-increase in C_{max} (C_{maxR}) and $AUC_{0-\infty}$ (AUC_R) with co-administration of crizotinib with 90% confidence interval (CI).

[b] Calculated predicted to observed pharmacokinetic parameter ratio.

[c] Simcyp simulation was performed using TDI parameters from either HLM or HSP.

Downloaded from dmd.aspetjournals.org at ASPET Journals on February 7, 2023

DMD Fast Forward. Published on November 5, 2012 as DOI: 10.1124/dmd.112.049114
This article has not been copyedited and formatted. The final version may differ from this version.

TABLE 4

Predicted fold-increase in midazolam $AUC_{0-\infty}$ by the static models using crizotinib steady-state average plasma concentration

TDI [a]	Crizotinib C_{ave} [b]		Predicted fold-increase in midazolam $AUC_{0-\infty}$			
			Static mathematical model			Simcyp R_{ss}
	ng/mL total	nM free	Liver	Gut	Liver + Gut	
HLM	255 [c]	53 [c]	11	1.6	17	−
	541 [d]	112 [d]	12	1.6	19	13
HSP	255 [c]	53 [c]	2.5	1.3	3.2	−
	271 [d]	56 [d]	2.6	1.3	3.3	2.3

−, not applicable

[a] Static mathematical models utilized TDI parameters from either HLM or HSP.

[b] Average steady-state plasma concentrations (C_{ave}) in total (ng/mL) and unbound (nM) forms were calculated from either the observed or Simcyp–predicted $AUC_{0-\tau}$ (listed in Table 2) divided by the dosing interval of 12 hours.

[c] Clinically observed crizotinib C_{ave} was used for the prediction of crizotinib-midazolam interaction with the static model.

[d] Simcyp-predicted crizotinib C_{ave} was used for the prediction of crizotinib-midazolam interaction with the static model.

Downloaded from dmd.aspetjournals.org at ASPET Journals on February 7, 2023

DMD Fast Forward. Published on November 5, 2012 as DOI: 10.1124/dmd.112.049114
This article has not been copyedited and formatted. The final version may differ from this version.

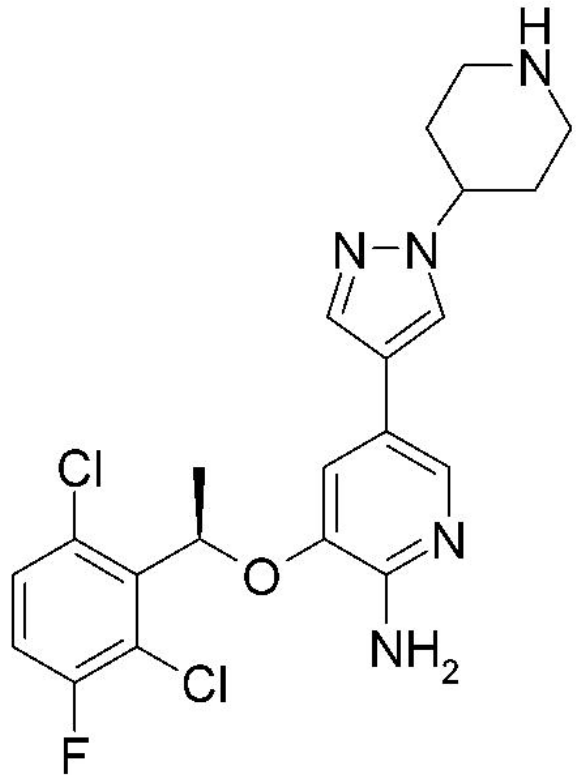

Figure 1

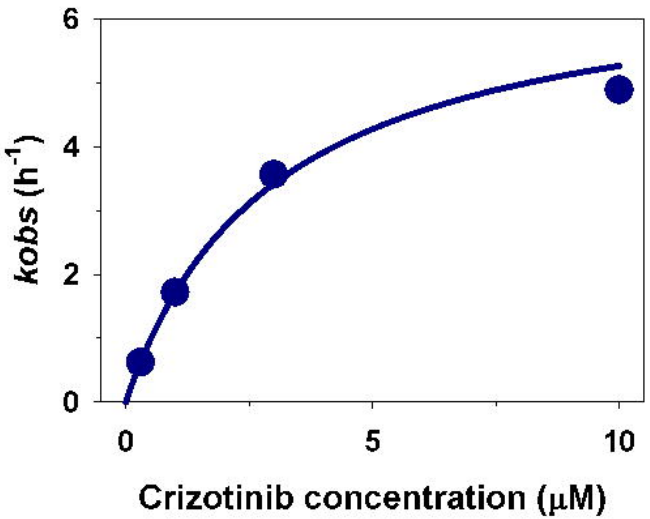

Figure 2

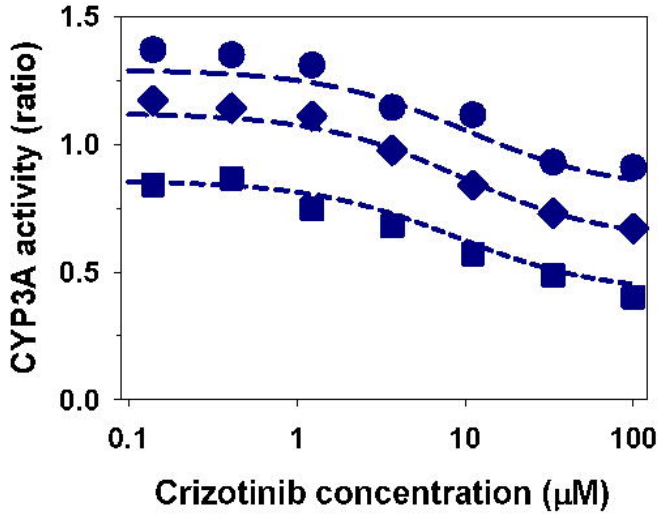
CYP3A activity (ratio)
1.5
1.0
0.5
0.0
0.1
1
10
100
Crizotinib concentration (μM)

Figure 3

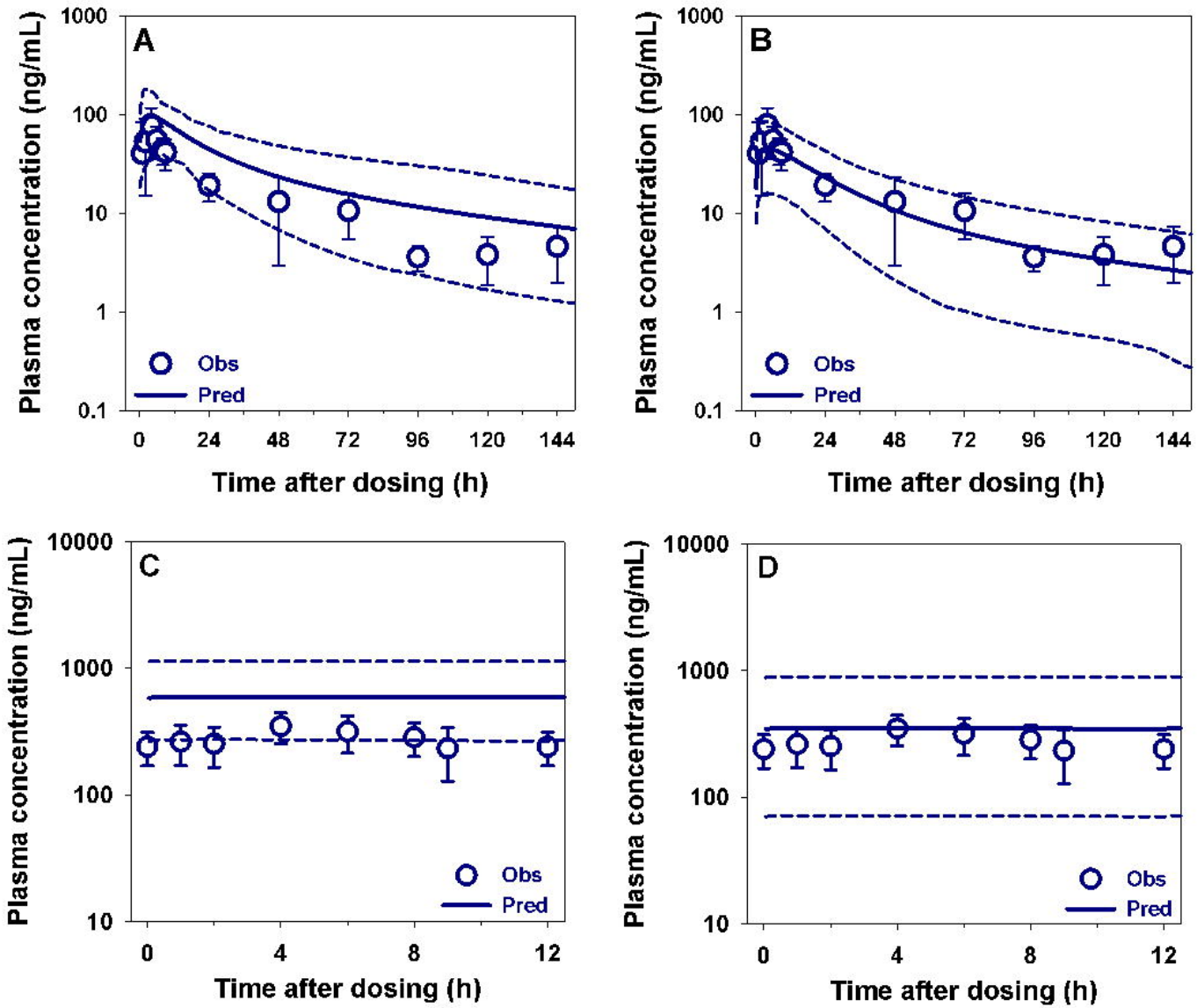
A
B
C
D
Plasma concentration (ng/mL)
Time after dosing (h)
Obs
Pred
1000
100
10
1
0.1
10000
0
24
48
72
96
120
144
4
8
12

Figure 4

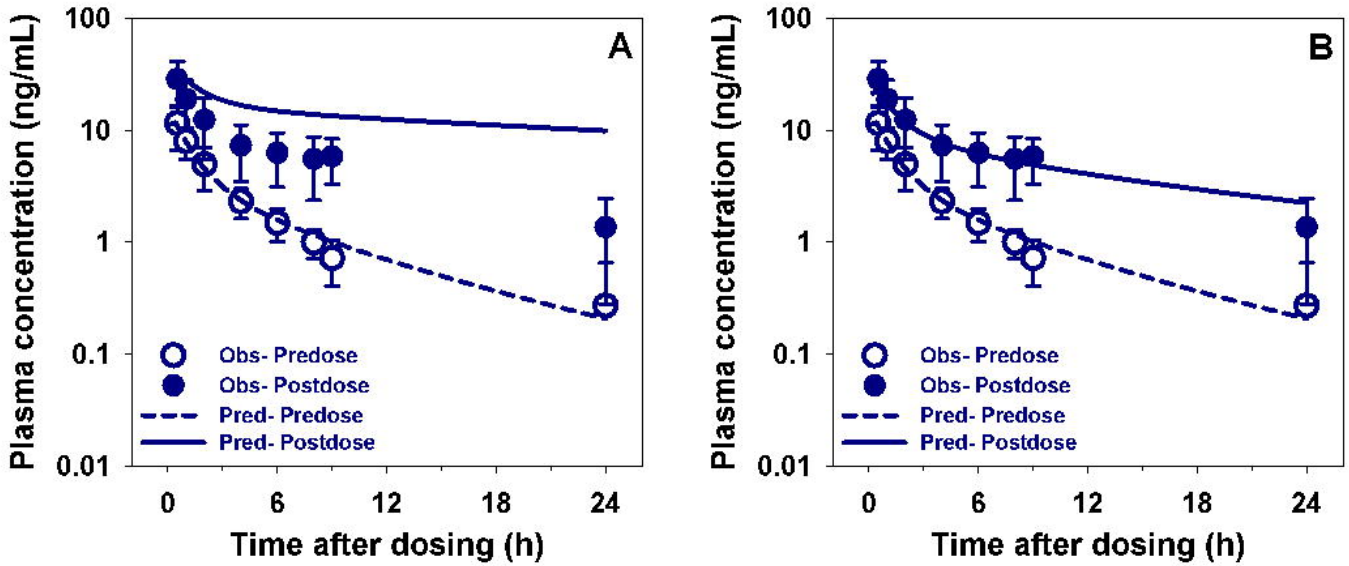
A
B
Plasma concentration (ng/mL)
100
10
1
0.1
0.01
0
6
12
18
24
Time after dosing (h)
Obs- Predose
Obs- Postdose
Pred- Predose
Pred- Postdose

Figure 5

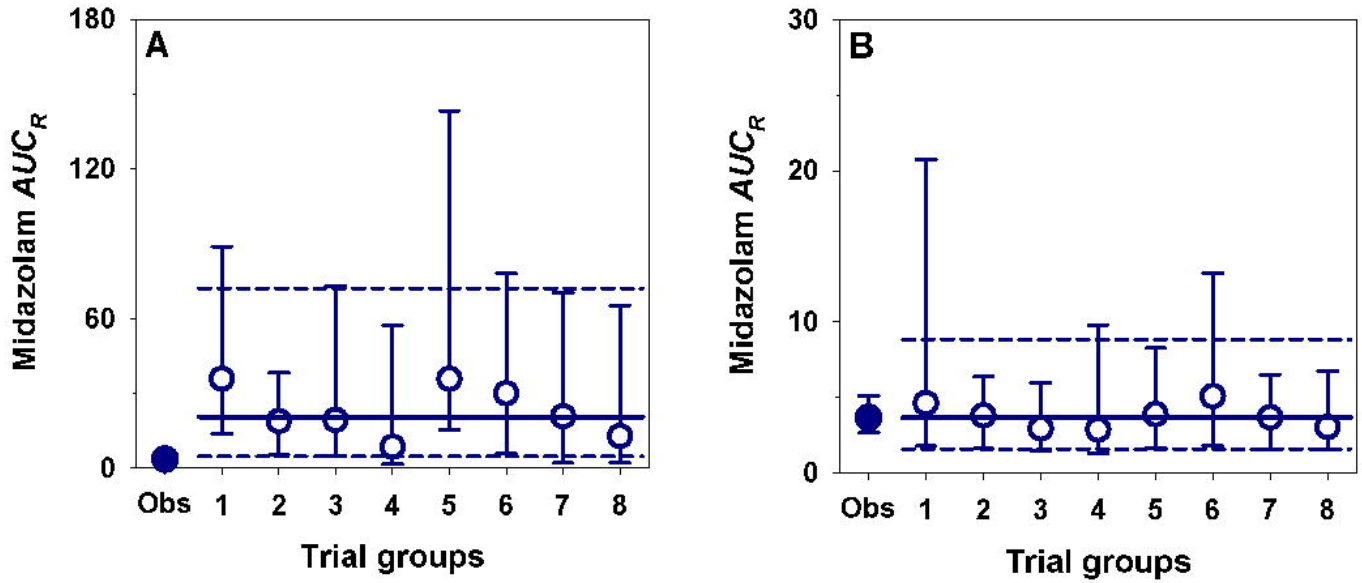
A
B
Midazolam AUC_R
180
120
60
0
30
20
10
Obs
1
2
3
4
5
6
7
8
Trial groups

Figure 6

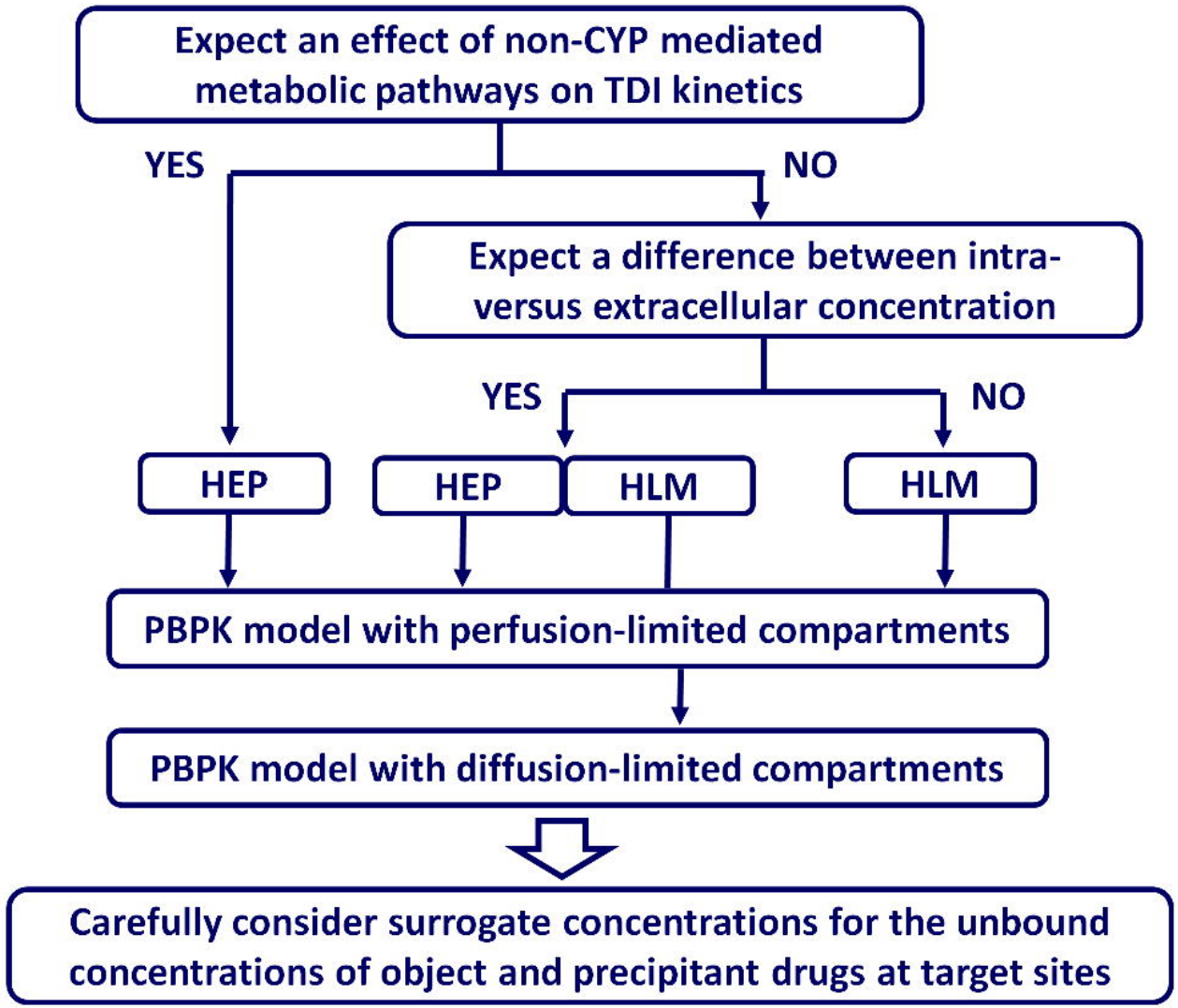
Expect an effect of non-CYP mediated metabolic pathways on TDI kinetics
YES
NO
Expect a difference between intra- versus extracellular concentration
YES
NO
HEP
HEP
HLM
HLM
PBPK model with perfusion-limited compartments
PBPK model with diffusion-limited compartments
Carefully consider surrogate concentrations for the unbound concentrations of object and precipitant drugs at target sites

Figure 7